Sensors & Transducers, Vol. 159, Issue 11, November 2013, pp. 379-384

www.sensorsportal.com

Sensors & Transducers

http://www.sensorsportal.com

Refractive Index Sensing by Using Nano Fiber Coupler

Liu Tiedong

Northeast Forestry University faculty of Landscape Architecture, Heilongjiang Harbin, China

Received: 13 November 2013 /Accepted: 26 November 2013 /Published: 30 November 2013

Abstract: Refractive index sensing by using nano fiber is popular researching direction which can find application in several of regions. In order to obtain the pressure, humidity, temperature and concentration in the detection environment, it is crucial that the detector is with nanoscale size and is sensitive to the change of the environment. In this paper, we present a refractive index sensor based on the coupler of the nano-fiber. Base on the mechanism of optical coupling, the proposed optical sensor can detect the local variation of the refractive index around the optical nano-fiber. By using finite difference time domain method, we numerically demonstrate the sensing capacity of the nano-optical coupler. The sensing mechanism underlying this method and the limitation of the propose sensor are also discussed. *Copyright © 2013 IFSA.*

Keywords: Optical sensing, Optical coupler, Nano-fiber.

1. Introduction

Optical fiber sensor, which can detect the refractive index variation of the environment, receives tremendous attention these years [1-8]. Because of its low cost and feasibility, it plays an important role in modern communication network, especially in the internet of things. The optical fiber sensors rely on the dependence between optical response and the optical environment. Variation in the optical environment would cause the change in optical path and thus the change of the optical phase. As a result, the optical response of the system would be different due to the coherent nature of the laser source. This kind of mechanism is the normal type of optical fiber sensor and is commonly used in the detection of biology sample.

There are different type of optical sensor which using the interference between two optical paths, for example, the Mach-Zehnder interferometer. The optical fiber Mach-Zehnder interferometer splits the incoming light into two beams and recombines at the final, giving rise interference that depends on the phase shift between two optical paths. Therefore, the phase shift, i.e. the variation of the refractive index in two optical paths, can be determined by the interference result and realize the refractive index sensing function.

Recently, nano-fiber receives extensive attention due to the subwavelength confinement of the optical wave and the extremely sensitive to the variation of refractive index surrounding the nano-fiber [9]. Because of lacking of cladding layer, the nano-fiber is using air as the cladding material and thus the refractive index surrounding the nano-fiber is critical to the dispersion of the light guiding in the nano-core. In other words, change in the background refractive index would lead to varying of the propagation constant of the optical mode and have an effect on the final optical transmission. We can therefore detect the local refractive index by the optical fiber system. Nano Mach-Zehnder interferometer based on the nano-fiber is one of the chose to facilitate the refractive index sensing in the nanoscale.

In this paper, we propose a simple optical sensor based on a nano-fiber couplear to realize refractive index sensing. Our geometry is two nano-fiber placed closely to permit tunneling between each of them. The working principle of our structure is relied on the evanescence coupling between nano-fibers. If the refractive index of the background medium is changed, the coupling condition would be changed at

the same time. It means that the optical phase acquired in the coupling process is related to the refractive index of the background medium. And this kind of mechanism can be used to detect the local variation of the refractive index.

The paper is organized as follows. Section 2 outlines the devices structure and the theoretical model. In Sec. 3, we present the numerical simulation result. Sec. 4 discuss the limitation of the sensing strategy and summaries the paper.

2. Devices Structure and Theoretical Model

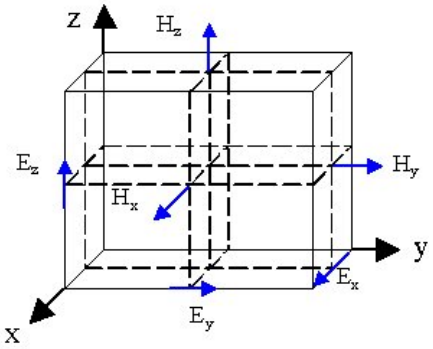

Fig. 1. Yee unit cell of the three dimensional FDTD method. Different components of the electromagnetic fields are labeled in the figure. Each of them is shifted compared with each other.

In order to fully model this kind of optical coupling structure, we chose the three dimensional finite difference time domain method (FDTD) [10]. In the time domain, the Maxwell equations can be written as:

$$\nabla \times \vec{H} = \frac{\partial \vec{D}}{\partial t} + \vec{J} \tag{1}$$

$$\nabla \times \vec{E} = -\frac{\partial \vec{B}}{\partial t} - \vec{J}_m, \tag{2}$$

where E is the electric field, H is the magnetic intensity, J is the current density, J_m is the magnetic (flux) density. They are function of temporal and spatial parameters. The constitutive relationships read as:

$$\vec{D} = \varepsilon \vec{E} \tag{3}$$

$$\vec{B} = \mu \vec{H} \tag{4}$$

$$\vec{J} = \sigma \vec{E} \tag{5}$$

$$\vec{J}_m = \sigma_m \vec{H}, \tag{6}$$

where μ is the permeability of vacuum, ε is the permittivity in vacuum, σ is the conductivity and σ_m is the permeability. They are scalars in isotropic medium while tensor in anisotropic medium. If there is no source in the space under consideration and ε , μ , σ and σ_m are temporal and spatial independent, Eq. (1) and (2) can be rewritten as:

$$\frac{\partial E_x}{\partial t} = \frac{1}{\varepsilon}\left(\frac{\partial H_z}{\partial y} - \frac{\partial H_y}{\partial z} - \sigma E_x\right) \tag{7}$$

$$\frac{\partial E_y}{\partial t} = \frac{1}{\varepsilon}\left(\frac{\partial H_x}{\partial z} - \frac{\partial H_z}{\partial x} - \sigma E_y\right) \tag{8}$$

$$\frac{\partial E_z}{\partial t} = \frac{1}{\varepsilon}\left(\frac{\partial H_y}{\partial x} - \frac{\partial H_x}{\partial y} - \sigma E_z\right) \tag{9}$$

$$\frac{\partial H_x}{\partial t} = \frac{1}{\mu}\left(\frac{\partial E_y}{\partial z} - \frac{\partial E_z}{\partial y} - \sigma_m H_x\right) \tag{10}$$

$$\frac{\partial H_y}{\partial t} = \frac{1}{\mu}\left(\frac{\partial E_z}{\partial x} - \frac{\partial E_x}{\partial z} - \sigma_m H_y\right) \tag{11}$$

$$\frac{\partial H_z}{\partial t} = \frac{1}{\mu}\left(\frac{\partial E_x}{\partial y} - \frac{\partial E_y}{\partial x} - \sigma_m H_z\right) \tag{12}$$

In order to discretize all the electromagnetic fields, K. S. Yee used the so-call Yee unit cell for the discretization of six electromagnetic fields shown in Eq. (7)-(12). Three electric field components are parallel to the sides of the cubic shown in Fig. (1). While the magnetic fields are perpendicular to the surface of the cubic, as are shown in the figure. There is a time step shift between the magnetic fields and the electric fields, as can be seen from Eq. (7)-(12). This kind of discretization is suitable for realizing the iteration algorithm of finite different time domain, which can quantitatively describe the evolution of the electromagnetic fields.

For the iteration convenience, each discrete spatial point of the Yee unit cell is labeled by the following method:

$$(i, j, k) = (i\Delta x, j\Delta y, k\Delta z) \tag{13}$$

While the electromagnetic function in such spatial point can be expressed as

$$f^n(i, j, k) = f\Big|_{i,j,k}^{n} = f(i\Delta x, j\Delta y, k\Delta z, n\Delta t) \tag{14}$$

where $\Delta x, \Delta y, \Delta z$ are the discretization step of the Yee unit cell, i, j, k are the integers, Δt is the time step. As can be seen from Fig. 1, the sample components of electric and magnetic fields can be taken as:

$$H_x^{n+1/2}(i,j+1/2,k+1/2), H_y^{n+1/2}(i+1/2,j,k+1/2),$$
$$H_z^{n+1/2}(i+1/2,j+1/2,k)$$

$$E_x^{n+1}(i+1/2,j,k), E_y^{n+1}(i,j+1/2,k),$$
$$E_z^{n+1}(i,j,k+1/2) \quad (15)$$

Because there are half time step difference between the spatial point of electric and magnetic fields, we use the central difference to approximate the first order derivative of the Maxwell equation:

$$\frac{\partial f(u)}{\partial u} = \frac{f(u+\Delta u/2) - f(u-\Delta u/2)}{\Delta u} + o(\Delta u^2), \quad (16)$$

where Δu is the step.
Therefore Eq. (7)-(12) can be written as:

$$E_x^{n+1}(i+\frac{1}{2},j,k) = C(i+\frac{1}{2},j,k)E_x^n(i+\frac{1}{2},j,k) + D(i+\frac{1}{2},j,k)\times \left\{ \begin{array}{l} \frac{H_z^{n+1/2}(i+\frac{1}{2},j+\frac{1}{2},k) - H_z^{n+1/2}(i+\frac{1}{2},j-\frac{1}{2},k)}{\Delta y} \\ \frac{H_y^{n+1/2}(i+\frac{1}{2},j,k+\frac{1}{2}) - H_y^{n+1/2}(i+\frac{1}{2},j,k-\frac{1}{2})}{\Delta z} \end{array} \right\} \quad (17)$$

$$H_x^{n+1/2}(i,j+\frac{1}{2},k+\frac{1}{2}) = C_m(i,j+\frac{1}{2},k+\frac{1}{2})H_x^{n-1/2}(i,j+\frac{1}{2},k+\frac{1}{2}) + D_m(i,j+\frac{1}{2},k+\frac{1}{2})\times \left\{ \begin{array}{l} \frac{E_y^n(i,j+\frac{1}{2},k+1) - E_y^n(i,j+\frac{1}{2},k)}{\Delta z} \\ \frac{E_z^n(i,j+1,k+\frac{1}{2}) - E_z^n(i,j,k+\frac{1}{2})}{\Delta y} \end{array} \right\} \quad (18)$$

$$E_y^{n+1}(i,j+\frac{1}{2},k) = C(i,j+\frac{1}{2},k)E_y^n(i,j+\frac{1}{2},k) + D(i,j+\frac{1}{2},k)\times \left\{ \begin{array}{l} \frac{H_x^{n+1/2}(i,j+\frac{1}{2},k+\frac{1}{2}) - H_x^{n+1/2}(i,j+\frac{1}{2},k-\frac{1}{2})}{\Delta z} \\ \frac{H_z^{n+1/2}(i+\frac{1}{2},j+\frac{1}{2},k) - H_z^{n+1/2}(i-\frac{1}{2},j+\frac{1}{2},k)}{\Delta x} \end{array} \right\} \quad (19)$$

$$H_y^{n+1/2}(i+\frac{1}{2},j,k+\frac{1}{2}) = C_m(i+\frac{1}{2},j,k+\frac{1}{2})H_y^{n-1/2}(i+\frac{1}{2},j,k+\frac{1}{2}) + D_m(i+\frac{1}{2},j,k+\frac{1}{2})\times \left\{ \begin{array}{l} \frac{E_z^n(i+1,j,k+\frac{1}{2}) - E_z^n(i,j,k+\frac{1}{2})}{\Delta x} \\ \frac{E_x^n(i+\frac{1}{2},j,k+1) - E_x^n(i+\frac{1}{2},j,k)}{\Delta z} \end{array} \right\} \quad (20)$$

$$E_z^{n+1}(i,j,k+\frac{1}{2}) = C(i,j,k+\frac{1}{2})E_z^n(i,j,k+\frac{1}{2}) + D(i,j,k+\frac{1}{2})\times \left\{ \begin{array}{l} \frac{H_y^{n+1/2}(i+\frac{1}{2},j,k+\frac{1}{2}) - H_y^{n+1/2}(i-\frac{1}{2},j,k+\frac{1}{2})}{\Delta x} \\ \frac{H_x^{n+1/2}(i,j+\frac{1}{2},k+\frac{1}{2}) - H_x^{n+1/2}(i,j-\frac{1}{2},k+\frac{1}{2})}{\Delta y} \end{array} \right\} \quad (21)$$

$$H_z^{n+1/2}(i+\frac{1}{2},j+\frac{1}{2},k) = C_m(i+\frac{1}{2},j+\frac{1}{2},k)H_z^{n-1/2}(i+\frac{1}{2},j+\frac{1}{2},k) + D_m(i+\frac{1}{2},j+\frac{1}{2},k)\times \left\{ \begin{array}{l} \frac{E_x^n(i+\frac{1}{2},j+1,k) - E_x^n(i+\frac{1}{2},j,k)}{\Delta y} \\ \frac{E_y^n(i+1,j+\frac{1}{2},k) - E_y^n(i,j+\frac{1}{2},k)}{\Delta x} \end{array} \right\} \quad (22)$$

where

$$C_m(i,j,k) = \frac{2\mu(i,j,k) - \sigma_m(i,j,k)\Delta t}{2\mu(i,j,k) + \sigma_m(i,j,k)\Delta t}$$
$$D_m(i,j,k) = \frac{2\Delta t}{2\mu(i,j,k) + \sigma_m(i,j,k)\Delta t}$$
$$C(i,j,k) = \frac{2\varepsilon(i,j,k) - \sigma(i,j,k)\Delta t}{2\varepsilon(i,j,k) + \sigma(i,j,k)\Delta t}$$
$$D(i,j,k) = \frac{2\Delta t}{2\varepsilon(i,j,k) + \sigma(i,j,k)\Delta t}$$

Therefore, Eq. (17)-(21) are consisted of the three dimensional finite difference time domain equations. As can be seen from these equations, the electromagnetic fields at any time are depended on the electric and magnetic fields at the last time step and the electromagnetic parameters. And we thus rewrite Eq. (17)-(21) as:

$$E_x^{n+1}(i,j,k) = C(i,j,k)E_x^n(i,j,k) + D(i,j,k)\cdot \left\{ \begin{array}{l} \frac{H_z^n(i,j,k) - H_z^n(i,j-1,k)}{\Delta y} \\ \frac{H_y^n(i,j,k) - H_y^n(i,j,k-1)}{\Delta z} \end{array} \right\} \quad (23)$$

$$H_x^n(i,j,k) = C_m(i,j,k)H_x^{n-1}(i,j,k) + D_m(i,j,k)\cdot \left\{ \begin{array}{l} \frac{E_y^n(i,j,k+1) - E_y^n(i,j,k)}{\Delta z} \\ \frac{E_z^n(i,j+1,k) - E_z^n(i,j,k)}{\Delta y} \end{array} \right\} \quad (24)$$

$$E_y^{n+1}(i,j,k)=$$

$$=C(i,j,k)E_y^n(i,j,k)+D(i,j,k)\cdot\left\{\begin{array}{l}\dfrac{H_x^n(i,j,k)-H_x^n(i,j,k)}{\Delta z}\\ \dfrac{H_z^n(i,j,k)-H_z^n(i-1,j,k)}{\Delta x}\end{array}\right\} \quad (25)$$

$$H_y^{n+1}(i,j,k)=$$

$$=C_m(i,j,k)H_y^{n-1}(i,j,k)+D_m(i,j,k)\cdot\left\{\begin{array}{l}\dfrac{E_z^n(i+1,j,k)-E_z^n(i,j,k)}{\Delta x}\\ \dfrac{E_x^n(i,j,k+1)-E_x^n(i,j,k)}{\Delta z}\end{array}\right\} \quad (26)$$

$$E_x^{n+1}(i,j,k)=$$

$$=C(i,j,k)E_x^n(i,j,k)+D(i,j,k)\cdot\left\{\begin{array}{l}\dfrac{H_z^n(i,j,k)-H_z^n(i,j-1,k)}{\Delta y}\\ \dfrac{H_y^n(i,j,k)-H_y^n(i,j,k-1)}{\Delta z}\end{array}\right\}$$

$$E_z^{n+1}(i,j,k)=$$

$$=C(i,j,k)E_z^n(i,j,k)+D(i,j,k)\cdot\left\{\begin{array}{l}\dfrac{H_y^n(i,j,k)-H_y^n(i-1,j,k)}{\Delta x}\\ \dfrac{H_x^n(i,j,k)-H_x^n(i,j-1,k)}{\Delta y}\end{array}\right\} \quad (27)$$

$$EH_z^{n+1}(i,j,k)=$$

$$=C_m(i,j,k)H_z^{n-1}(i,j,k)+D_m(i,j,k)\cdot\left\{\begin{array}{l}\dfrac{E_x^n(i,j+1,k)-E_x^n(i,j,k)}{\Delta y}\\ \dfrac{E_y^n(i+1,j,k)-E_y^n(i,j,k)}{\Delta x}\end{array}\right\} \quad (28)$$

which is suitable for coding and solving by computer. As can be seen from the upper discussion, the three dimensional finite difference time domain method is based on the finite difference approximation which numerically solves the curl equation. At the same time, we need the algorithm to be stable and reliable. General conditions for realizing stable calculation are summarized as follow:

1) The grid size is smaller than one-tenth of the minimum wavelength considered in the computation.
2) The courant stable condition should be fulfilled.

$$\Delta t \le \frac{1}{C_{\max}\sqrt{\dfrac{1}{(\Delta x)^2}+\dfrac{1}{(\Delta y)^2}+\dfrac{1}{(\Delta z)^2}}},$$

where C_{max} is the maximum phase velocity in the electromagnetic medium.

3. Simulation Result

The geometry under consideration is shown in Fig. 2 where two nano-fibers are arranged with subwavelength gap d. The diameter of the nano-fiber is 600nm. Such kind of nano-fiber is fabricated by flameheated treatment which can produce fiber with diameter down to nanoscale [11]. Our structure is based on the combination of two nano-fibers placed closed to each other. The distance between two fibers is d as is shown in Fig. 2.

Our motivation is based on the guide mode tunneling of a nano-fiber. As can be seen from Fig. 2, when the light source is injected at one side of the fiber end, it would have evanescence wave around the surface because of the total internal reflection at the fiber-air interface. If there is another fiber placing close to the infected fiber, couple tunneling occurs and the energy flow can be redirected into the second fiber. Such kind of process is relied on the optical coupling between modes in two nano-fibers. It means that the environment around the fiber coupler would have an effect on the coupling result. As far as we understand, changing the refractive index of the background medium would definitely change the guiding condition of the optical modes in the nano-fiber. Variation of the background refractive index would change the optical phase delay when the tunneling is occurs. As a result, we can use such simple architecture to monitor the variation of the refractive index.

We choose the three dimensional finite difference time domain method proposed above to demonstrate the sensing performance of the nano-fiber coupler. By changing the refractive index of the background medium, the situation of background varying is mimicked. The numerically calculated results are shown in Fig. 3 (a). It is obviously that the transmission spectrum is different referring to different background medium. When the refractive index of the background medium is changed from n=1.1 to n=1.5, the transmission spectrums suffers from transformation which results from the feedback of the refractive index in the background. In order to visualize the working mechanism of the optical nano-fiber coupler, we calculate the electromagnetic field evolutions of this sensor, as are shown in Fig. 3 (b) and (c). The color scale is referred to the electromagnetic power of the system. It can be seen from the results that there are distinct propagation results at different wavelength. Light signal can be transmitted through the nano-fiber coupler near the telecom wavelength 1550 nm (marked b in Fig. 3 (a)). While at the frequency (marked a in Fig. 3 (a)), the input light cannot enter the second nano-fiber due to the tunneling condition cannot be fulfilled. These kinds of effects demonstrated our motivation exactly.

In other words, we can therefore detect the refractive index of the background and thus realize the function of refractive index sensing.

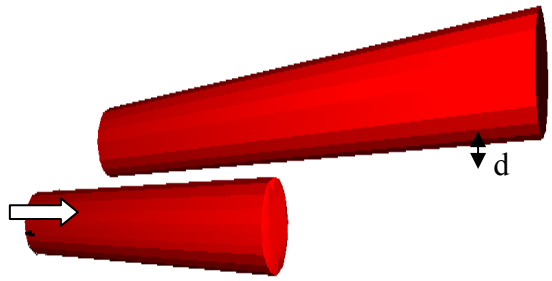

Fig. 2. Geometry of the optical nano fiber coupler with the distance d. The diameter of the nano-fiber is 600nm. n is the refractive index of the background medium surrounding the nano fiber coupler while N is the refractive index of the nano-fiber (N=1.6). By monitoring the transmission spectrum at the output port, we can monitor the variation of the refractive index in the background medium, as discussed in the context.

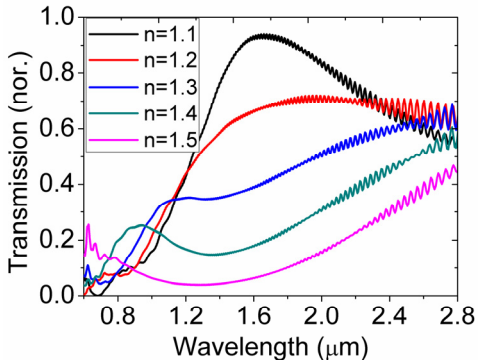

(a)

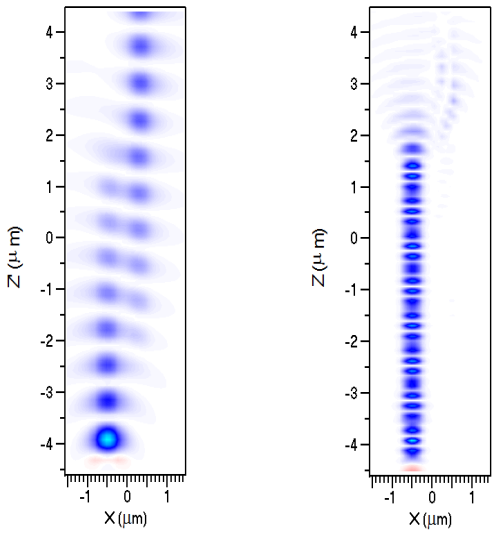

(b) (c)

Fig. 3. (a) Transmission spectrum calculated by the three dimensional finite difference time domain numerical experiments. Different colors are referred to different background refractive index as are shown in the inset. (b) Power distribution at the wavelength marked b in Fig. 3 (a). The cross-section view of the nano-fiber coupler is taken at the center of the coupler. (c) Power distribution at the wavelength marked a in Fig. 3 (a). The X-Z aspect ratio is 1:1.

4. Conclusions

Our sensing system has some drawback which could have influence on the performance of the proposed device. One of them is the ruggedness of the coupler. It means that particular mechanical treatment should be taken to enhance the stability of our nano-fiber coupler sensor. At the same time, if the refractive index of the background medium

exceeds the refractive index of the nano-fiber, the optical guiding condition cannot be fulfilled and thus the guiding of the light wave signal cannot be realized. As a result, new material with high refractive index could be one of the solution conquer this problem.

In conclusion, a nano-fiber coupler based sensor which is suitable for detecting refractive index in the nanoscale is proposed and demonstrated numerically. Relying on the evanescence tunneling, the optical fiber coupler can detect a change of the refractive index in the background. According to the change of the transmission spectrum, we can in turn determine the variation of the refractive index in the environment. We expect this kind of sensor could be used in biosensing and chemical sensing system and our motivation can be generalized to other similar system.

5. Acknowledgements

The work was supported by "the Fundamental Research Funds for the Central Universities" DL12BA15.

References

[1]. J. Mathew, Y. Semenova, G. Farrell, Relative Humidity Sensor Based on an Agarose-Infiltrated Photonic Crystal Fiber Interferometer, *IEEE Journal of Selected Topics in Quantum Electronics*, Vol. 18, Issue 5, 2012, pp. 1553-1559.

[2]. B. H. Lee, Y. Liu, S. B. Lee, S. S. Choi, and J. N. Jang, Displacements of the resonant peaks of a long-period fiber grating induced by a change of ambient refractive index, *Opt. Lett.,* Vol. 22, 1997, pp. 1769-1771.

[3]. H. Y. Choi, M. J. Kim and B. H. Lee, All-fiber Mach-Zehnder type interferometers formed in photonic crystal fiber, *Opt. Express*, Vol. 15, 2007, pp. 5711-5720.

[4]. P. F. Wang, Y. Semenova, Q. Wu, and G. Farrell, Microw., A bend loss–based singlemode fiber microdisplacement sensor, *Opt. Technol. Lett*, Vol. 52, 2010, pp. 2231-2235.

[5]. Z. Y. Wang and S. Ramachandran, Ultrasensitive long-period fiber gratings for broadband modulators and sensors, *Opt. Lett*, Vol. 28, 2003, pp. 2458-2460.

[6]. X. Shu, B. A. L. Gwandu, Y. Liu, L. Zhang, and I. Bennion, Sampled fiber Bragg grating for simultaneous refractive-index and temperature measurement, *Opt. Lett,* Vol. 26, 2001, pp. 774-776, .

[7]. R. Jha, J. Villatoro, G. Badenes and V. Pruneri, Refractometry based on a photonic crystal fiber interferometer, *Opt. Lett.,* Vol. 34, 2009, pp. 617-619.
[8]. J. Villatoro, V. P. Minkovich, V. Pruneri and G. Badenes, Simple all-microstructured-optical-fiber interferometer built via fusion splicing, *Opt. Express*, Vol. 15, 2007, pp. 1491-1496.
[9]. Z. L. Wang, R. P. P. Gao, J. L. Gole and J. D. Stout, Silica nanotubes and nanofiber arrays, *Advanced Materials,* Vol. 12, 2000, pp. 1938-1940.
[10]. Allen Taflove and Susan C., Hagness computational Electrodynamics: The Finite-Difference Time-Domain Method, 3rd ed., *Artech House Publishers*, 2005.
[11]. Lee, S., Cunnington, G., Conduction and Radiation Heat Transfer in High-Porosity Fiber Thermal Insulation, *Journal of Thermophysics Heat and Transfer,* Vol. 14, 2000, pp. 121-136.